

Integrated Multimodal Interaction Using Texture Representations[☆]

Auston Sterling, Ming C. Lin

University of North Carolina at Chapel Hill

Abstract

In this paper, we explore texture mapping as a unified representation for enabling realistic multimodal interaction with finely-detailed surfaces. We show how both normal maps and relief maps can be adopted as unified representations to handle collisions with *textured* rigid body objects, synthesize complex sound effects from long lasting collisions and perform rendering of haptic textures. The resulting multimodal display system allows a user to see, hear, and feel complex interactions with textured surfaces. By using texture representations for seamlessly integrated multimodal interaction instead of complex triangular meshes otherwise required, this work is able to achieve up to 25 times performance speedup and reduce up to six orders of magnitude in memory storage. We further validate the results through user studies to demonstrate the effectiveness of texture representations for integrated multimodal display.

1. Introduction

In computer graphics, texture mapping has been one of the most widely used techniques to improve the visual fidelity of objects while significantly accelerating the rendering performance. There are several popular texture representations, such as displacement maps [1], bump mapping with normal maps [2, 3], parallax maps [4, 5], relief maps [6, 7], etc., and they are used mostly as “imposters” for rendering static scenes. These textures are usually mapped onto objects’ surfaces represented with simplified geometry. The fine details of the objects are visually encoded in these texture representations. By replacing the geometric detail with a texture equivalent, the resulting rendered image can be made to appear much more complex than its underlying polygonal geometry would otherwise convey. These representations also come with a significant increase in performance: texture maps can be used for real-time augmented and virtual reality (AR/VR) applications on low-end commodity devices.

Sensory conflict occurs when there is a mismatch between information perceived through multiple senses and can cause a break in immersion in a virtual environment. When textures are used to represent complex objects with simpler geometry, sensory conflict becomes a particular concern. In an immersive virtual environment, a user may see a rough surface of varying heights and slopes represented by its texture equivalent mapped to a flat surface. In the real world, objects behave very differently when bouncing, sliding, or rolling on bumpy or rough surfaces than they do on flat surfaces. With visually complex detail and different, contrasting physical behavior due to the simple flat surface, sensory conflict can easily occur—breaking the sense of immersion in the virtual environment. In order to

capture such behaviors, the geometry used in a physics simulator would usually require a fine triangle mesh with sufficient surface detail, but in most cases a sufficiently fine mesh is unavailable or would require prohibitive amounts of memory to store.

Since the given texture maps contain information about the fine detail of the mapped surface, it is possible to use that information to recreate the behavior of the fine mesh. Haptic display and sound rendering of textured surfaces have both been independently explored [8, 9], but texture representations of detail have not been previously used for visual simulation of dynamic behavior due to collisions and contacts between rigid bodies. For example, the system for sound rendering of contacts with textured surfaces [9] displays a pen sliding smoothly across highly bumpy surfaces. While the generated sound from this interaction is dynamic and realistic, the smooth *visual* movement of the pen noticeably does not match the texture implied by the sound. In order to minimize sensory conflict, it is critical to present a unified and seamlessly integrated multimodal display to users, ensuring that the sensory feedback is consistent across the senses of sight, hearing, and touch for both coarse and fine levels of detail.

Motivated by the need to address the sensory conflict due to the use of textures in a multimodal virtual environment, we previously examined the use of normal mapping as a unified representation of fine detail for sight, hearing, and touch [10]. In this paper, we explore both normal maps and relief maps for integrated multimodal display. The main results of this work include:

- A new effective method for visual simulation of physical behaviors for rigid objects textured with normal maps;
- A seamlessly integrated multisensory interaction system using normal maps;

[☆]<http://gamma.cs.unc.edu/MultiDispTexture>

- An extended system using relief maps;
- Evaluation and analysis of texture-based multimodal display and their effects on task performance; and
- Evaluation of perceptual differences between normal and relief map representations.

The rest of the paper is organized as follows. We first discuss why we have selected normal and relief maps as our texture representations for multimodal display. We then describe how each mode of interaction can specifically use normal maps to improve perception of complex geometry (Sec. 3). We highlight the behavior of virtual objects as they interact with a large textured surface, and describe a new method to improve visual perception of the simulated physical behaviors of colliding objects with a textured surface using normal maps. We also demonstrate how to use the same normal maps in haptic display and sound rendering of textured surfaces. We describe how the additional depth information in relief maps can be used to improve each mode of interaction (Sec. 4).

We have implemented a prototype multimodal display system using normal and relief maps and performed both qualitative and quantitative evaluations of its effectiveness on perceptual quality of the VR experience and objective measures on task completion (Sec. 5). A user study suggests that normal maps can serve as an effective, unified texture representation for seamlessly integrated multi-sensory display and the resulting system generally improves task completion rates with greater ease over use of a single modality alone. A second user study suggest that relief maps are also an effective representation of fine detail, with an improvement in sensory cohesiveness over normal maps.

2. Previous Work

Normal maps and relief maps are used throughout this paper as representations of fine detail of the surface of objects. Normal maps were originally introduced for the purposes of bump mapping, where they would perturb lighting calculations to make the details more visibly noticeable [2]. Relief mapping uses both depths and normals for more complex shading [6, 7]. Numerous other texture mapping techniques exist as well. Displacement mapping, parallax mapping, and a number of more recent techniques use height maps to simulate parallax and occlusion [1, 4, 5]. A recent survey goes into more detail about many of these techniques [11]. Mapping any of these textures to progressive meshes can preserve texture-level detail as the level-of-detail (LOD) of the mesh shifts [3].

Height maps mapped to object surfaces have been used to modify the behavior of simple collisions in rigid-body simulations [12]. We are not aware of similar work done using normal maps aside from our own.

In haptic rendering, a 3D object’s geometries and textures can be felt by applying forces based on point-contacts with the object [13, 14]. Complex objects can also be simplified, with finer detail placed in a displacement map and referenced to produce accurate force *and torque* feedback on a probing object [8].

The mapping of both normal and displacement maps to simplified geometry for the purposes of haptic feedback has also been explored [15]. Dynamic deformation textures, a variant of displacement maps, can be mapped to create detailed objects with a rigid center layer and deformable outer layer. The technique has been extended to allow for 6-degree-of-freedom (DOF) haptic interaction with these deformable objects [16]. A common approach to force display of textures is to apply lateral force depending on the gradient of a height map such that the user of the haptic interface feels more resistance when moving “uphill” and less resistance when moving “downhill” [17, 18]. Our approach to haptic rendering of textures applies force feedback to simulate the presence of planes which reproduce this effect, and similarly we use a simplified model for interaction with dynamic rigid-body objects.

Modal analysis and synthesis are commonly used techniques for synthesizing realistic sound [19]. Modal synthesis has been integrated with rigid-body physics simulators in order to produce contact sounds that synchronize with collision events. To handle objects with arbitrary geometry, they can be decomposed with finite element methods [20]. Further speed optimizations can be made based on psychoacoustics, such as mode compression and truncation [21]. We synthesize transient impact sounds by directly using this technique.

Sounds created by long-lasting contacts between objects require some additional effort. Fractal noise is a common way of representing the small impacts generated during rolling and scraping [22]. We perform sound synthesis for lasting sounds by using the framework for synthesizing contact sounds between textured objects [9]. This work introduced a multi-level model for lasting contact sounds combining fractal noise with impulses collected from the normal maps on the surfaces of the objects. This application of normal maps to sound generation without similar application to rigid-body dynamics causes noticeable sensory conflict between the produced audio and visible physical behavior.

3. Overview and Texture Map Representation

Our system uses three main components to create a virtual scene where a user can experience through multiple modalities of interaction. A rigid body physics simulator controls the movement of objects. The only form of user input is through a haptic device, which also provides force feedback to stimulate the sense of touch. Finally, modal sound synthesis is used to dynamically generate the auditory component of the system. In this section, we briefly cover the details of texture mapping, discuss haptic illusions and justify the use of texture representations, then describe each of these components using normal maps as the representation of detail. The relief map representation is covered in greater detail in Section 4.

3.1. Normal and Relief Maps

Normal maps are usually stored as RGB images, with the color values encoding vectors normal to the details of the surface they are mapped to. Refer to Figure 1 for an example. It is

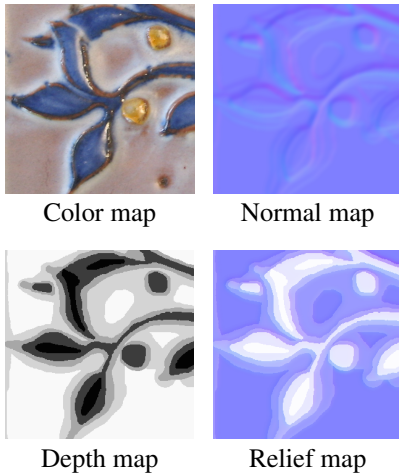


Figure 1: Texture map example. RGB values encode normal vectors in each texel. In relief maps, the alpha value encodes depth information.

171 common practice to create normal maps directly corresponding
 172 to a color map, such that the color map can be referenced at a lo-
 173 cation to get a base color and the normal map can be referenced
 174 at the same location for the corresponding normal vector.

175 Relief mapping is a technique for rendering textured sur-
 176 faces using additional depth information. It is usually imple-
 177 mented on GPUs and can be briefly described as computing
 178 intersections with the height-field defined by the depth values
 179 using rays from the camera to each pixel [7]. Ray casting lets
 180 relief-mapped surfaces properly handle self-occlusion, and ex-
 181 tra ray casts from a light source enable self-shadowing. Since
 182 rays are cast from the camera, proper perspective is maintained
 183 as the camera looks at the textured surface from different angles.
 184 Our surfaces are rendered using relief mapping, so we refer to
 185 their textures as “relief maps”, though the same texture could
 186 be used for parallax occlusion mapping or for displacements on
 187 GPU-tessellated surfaces.

188 Our relief maps contain their depth information in the al-
 189 pha channel of the image. In the alpha channel, a value of
 190 zero (black, entirely transparent) means the texel is at its high-
 191 est, exactly along the geometry of the mapped object. Larger
 192 values (tending towards white/visible) indicate that the texel is
 193 recessed inside the object. Much like sculpted relief artwork,
 194 relief maps can only cut into the surface; they cannot raise a
 195 texel outside the object’s geometry. The maximum depth as a
 196 percentage of mapped object dimensions can be set individually
 197 for each relief map.

198 Depending on the resolution of the texture image and the
 199 surface area of the object it is mapped to, a normal or relief
 200 map can provide very fine detail about the object’s surface. As
 201 we describe in this paper, this detail—while still an approxima-
 202 tion of a more complex surface—is sufficient to replicate other
 203 phenomena requiring knowledge of fine detail.

204 3.2. Design Consideration

205 Next we discuss various consideration in choosing texture
 206 maps as our representation of fine detail, beginning with a dis-
 207 cussion on haptic perception.

208 3.2.1. Haptic Illusions

209 Perceptual illusions, including visual, haptic and auditory,
 210 have been explored in virtual reality for immersing users in
 211 computer generated environments through multi-sensory dis-
 212 play. For example, bump mapping can be regarded as a vi-
 213 sual illusion where a user who is expecting to see depth in a
 214 bump-mapped surface may interpret the shading as depth. Hap-
 215 tic illusions can be roughly defined as when a haptic stimulus
 216 is applied under specific conditions that change the perception
 217 of that stimulus. A classic example is the size-weight illusion
 218 in which a participant lifts two boxes of equal weight and un-
 219 equal sizes and perceives the smaller box to be heavier. There
 220 are many types of haptic illusions, which have been well docu-
 221 mented and catalogued [23].

222 There are some real-world examples of haptic illusions which
 223 are relevant for simulating slope and depth. In the “curved
 224 plate” illusion, a flat edge rolled over a fingertip at about 1 Hz
 225 produces the sensation that the edge is curved. As described ear-
 226 lier, previous work on simulating haptic textures also relies on
 227 haptic illusions: applying only lateral forces to a haptic probe
 228 can create the sensation of a vertical height difference.

229 In these illusions, the changing direction of normal force
 230 creates the illusion of curvature. That is, *the normal vector is an*
 231 *important haptic cue for curvature*. Texture maps with normal
 232 vectors provide exactly that information, and therefore should
 233 be able to simulate the curvature of a more complicated surface
 234 through haptic illusions. This observation forms the hypothesis
 235 of our exploration of texture representations.

236 3.2.2. Choice of Representation

237 On top of providing an important haptic cue, normal vectors
 238 have additional advantages over alternative options. Using very
 239 high-resolution geometry would automatically produce many
 240 of the desired effects, but the performance requirements for *in-*
 241 *teractive* 3D applications significantly reduces their viability in
 242 our early deliberation. This is especially important to consider
 243 in AR and VR applications, where real-time performance must
 244 be maintained while possibly operating on a low-end mobile
 245 phone or head mounted display.

246 Other texture map information may also be considered, such
 247 as height (or displacement) maps. For sound, Ren et al. [9] used
 248 normal maps because the absolute height does not affect the re-
 249 sulting sound; it is the change in normal which causes a single
 250 impulse to produce meso-level sound. With regard to force dis-
 251 play of textured surfaces, the Sandpaper system [18] has been
 252 a popular and efficient method for applying tangential forces to
 253 simulate slope based on a height map. Using normal vectors we
 254 can instead scale a sampled normal vector to produce the same
 255 normal and tangential forces. Rigid body collision response
 256 also depends entirely on normal vectors.

257 Since each component of the system depends directly on
 258 the normals, a normal map representation emerges as the nat-
 259 ural choice. An added convenience is that normal maps are
 260 widely supported (including mobile games) and frequently in-
 261 cluded alongside color maps. Although normal maps contain
 262 the most important cues for multimodal interaction, we would

263 like to evaluate how much benefit is gained from combining nor-
 264 mals with depth information. Relief mapping uses both for vi-
 265 sual rendering and has become more common alongside GPUs,
 266 so relief maps provide a useful starting point for considering
 267 depth in multimodal interaction with textures. The application
 268 needs, the performance requirement, and the wide availability
 269 and support on commodity systems all contribute to our adop-
 270 tion of normal maps and relief maps as the mapping techniques
 271 in this work.

272 3.3. Rigid Body Dynamics

273 In order to simulate the movement of objects in the virtual
 274 scene, we use a rigid body dynamics simulator. These simula-
 275 tors are designed to run in real time and produce movements of
 276 rigid objects that visually appear believable.

277 Rigid body dynamics has two major steps: collision detec-
 278 tion and collision response. Collision detection determines the
 279 point of collision between two interpenetrating objects as well
 280 as the directions in which to apply force to most quickly sepa-
 281 rate them. Modifying the normals of an object, as we do with
 282 normal maps, does not affect whether or not a collision occurs.
 283 This is a significant limitation of a normal map representation
 284 without any height or displacement information.

285 There are numerous algorithms for collision resolution, which
 286 determines how to update positions and/or velocities to sepa-
 287 rate the penetrating objects. In impulse-based approaches, col-
 288 lisions are resolved by applying an impulse in the form of an in-
 289 stantaneous change in each objects' velocity. Considering a sin-
 290 gle object's velocity vector \mathbf{v} , $\Delta\mathbf{v}$ is chosen to be large enough
 291 so that the objects separate in the subsequent timesteps. The
 292 change in velocity on an object with mass m is computed by
 293 applying a force f over a short time Δt in the direction of the
 294 geometric normal \mathbf{n}_g of the other colliding object:

$$\Delta\mathbf{v} = \frac{f\Delta t}{m}\mathbf{n}_g \quad (1)$$

295 This process is highly dependent on the normal vectors of each
 296 object, and other collision resolution approaches have this same
 297 dependency.

298 3.3.1. Modifying Collision Behavior with Normal Maps

299 We focus on simulating collisions between small dynamic
 300 objects and large textured surfaces whose details would have a
 301 large effect on the dynamic object. To get an intuitive under-
 302 standing of the behavior we seek to replicate, imagine a marble
 303 rolling on a brick-and-mortar floor. When the marble rolls to
 304 the edge of a brick, the expected behavior would be for it to fall
 305 into the mortar between bricks and possibly end up stuck at the
 306 bottom.

307 The level of detail needed to accurately recreate these dy-
 308 namics with a conventional rigid body physics engine is too
 309 fine to be interactively represented with a geometric mesh, es-
 310 pecially with large scenes in real-time applications. A normal
 311 map contains the appropriate level of detail and is able to repre-
 312 sent the flat brick tops and rounded mortar indentations.

313 In order to change the behavior of collisions to respect fine
 314 detail, our solution is to modify the contact point and contact

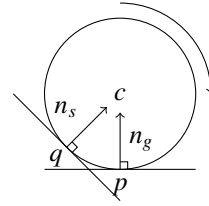


Figure 2: Contact point modification on a rolling ball: given the contact point \mathbf{p} and sampled normal \mathbf{n}_s , we want to simulate the collision at point \mathbf{q} .

315 normal reported by the collision detection step. This is an extra
 316 step in resolving collisions, and does not require any changes to
 317 the collision detection or resolution algorithms themselves.

318 The contact normal usually comes from the geometry of the
 319 colliding objects, but the normal map provides the same infor-
 320 mation with higher resolution, so our new approach uses the
 321 normal map's vectors instead. Given the collision point on the
 322 flat surface, we can query the surface normal at that point and
 323 instruct the physics engine to use this perturbed normal instead
 324 of the one it would receive from the geometry. One side effect
 325 of using the single collision point to find the perturbed normal
 326 is that it treats the object as an infinitely small probe.

327 3.3.2. Rolling Objects and Collision Point Modification

328 There is a significant issue with this technique when simu-
 329 lating rolling objects. Refer to Figure 2 for an example. Two
 330 planes are shown, the horizontal one being the plane of the
 331 coarse geometry and the other being the plane simulated by the
 332 perturbed normal. Note that the contact points with the rolling
 333 ball differ when the plane changes. The vector \mathbf{n}_s shows the di-
 334 rection of the force we would ideally like to apply. If we were
 335 to apply that force at the original contact point \mathbf{p} , the angular
 336 velocity of the sphere would change and the ball would begin
 337 to roll backwards. In practice, this often results in the sphere
 338 rolling in place when it comes across a more extreme surface
 339 normal. Instead, we use the sphere radius r , the perturbed sur-
 340 face normal \mathbf{n}_s , and the sphere center \mathbf{c} to produce the modified
 341 contact point \mathbf{q} :

$$\mathbf{q} = \mathbf{c} - (r\mathbf{n}) \quad (2)$$

342 This modification applies the force directly towards the center
 343 of mass and causes no change in angular velocity, but is less
 344 accurate for large spheres and extreme normal perturbations.

345 This contact point modification is important for perceptu-
 346 ally believable rolling effects. Shapes other than spheres do not
 347 have the guarantee that the contact point will be in the direction
 348 of the $\mathbf{c} - \mathbf{n}$ vector, so this does not apply in the general case.
 349 Generally, we can simply modify the normal without changing
 350 the contact point. In the case of relief maps, the true collision
 351 points and contact normals can be determined, so this correc-
 352 tion is unnecessary.

353 3.4. Haptic Interface

354 We have designed our system to use a PHANToM Desktop
 355 haptic device [24]. This device can measure 6-DOF motion:
 356 three translational and three rotational, but only display 3-DOF

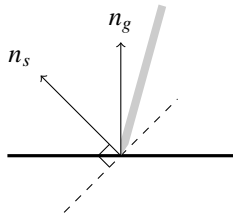


Figure 3: Haptic force is applied in the direction of the sampled normal \mathbf{n}_s instead of the geometric normal \mathbf{n}_g .

357 forces (i.e. no torques). We have chosen to represent the PHAN-
 358 ToM as a pen inside the virtual environment, which matches
 359 the scale and shape of the grip. While we could use forces de-
 360 termined by the rigid-body physics engine to apply feedback,
 361 the physics update rate (about 60 Hz) is much lower than the
 362 required thousands of Hz needed to stably simulate a hard sur-
 363 face.

364 We simulate the textured surface by projecting the tip of the
 365 PHANToM Desktop grip onto the surface in the direction of the
 366 coarse geometry’s normal. The fine surface normal is queried
 367 and interpolated from nearby normal map vectors. The PHAN-
 368 ToM simulates the presence of a plane with that normal and
 369 the projected surface point. Given the normal vector sampled
 370 from the normal map \mathbf{n}_s and pen tip position projected onto the
 371 surface \mathbf{p} , the equation modeling this plane is:

$$(\mathbf{n}_s \cdot (x, y, z)) - (\mathbf{n}_s \cdot \mathbf{p}) = 0 \quad (3)$$

372 The PHANToM now needs to apply the proper feedback force
 373 to prevent the pen’s tip from penetrating into the plane. This
 374 is accomplished using a penalty force, simulating a damped
 375 spring pulling the point back to the surface. Using the modi-
 376 fied normal vector, the simulated plane serves as a local first
 377 order approximation of the surface. Note that while the slopes
 378 of the planes produced by the PHANToM can vary significantly
 379 based on the normal map, at the position of the pen the plane
 380 will coincide with the surface. This is illustrated in Figure 3,
 381 where the simulated plane intersects the geometric plane at the
 382 collision point. This creates an illusion of feeling a textured sur-
 383 face while keeping the pen in contact with the flat underlying
 384 surface geometry.

385 With this technique, stability can be concern in some cases.
 386 Most noticeably, in steep and narrow V-shaped valleys, a user
 387 pushing down on the surface might cause the tip of the pen to
 388 oscillate between the valley sides. Users sliding the pen rapidly
 389 across bumpy surfaces may also feel forces that are stronger and
 390 more abrupt than they would expect. We have mainly mitigated
 391 these concerns by smoothing the normal maps and scaling down
 392 the penalty forces. A side effect is that the surfaces end up
 393 feeling slightly smoother and softer, though we have found this
 394 an acceptable tradeoff for improved stability.

395 We use a simplified model to interact with dynamic objects.
 396 The PHANToM’s corresponding pen appearance in the environ-
 397 ment is added as an object in the rigid-body physics simulator.
 398 Whenever this pen comes in contact with a dynamic object, the
 399 physics simulator computes the forces on the objects needed to
 400 separate them. We can directly apply a scaled version of this
 401 force to the haptic device. This ignores torque as our 3-DOF

402 PHANToM can only apply translational forces. This approach
 403 is fast, simple, and lets the user push and interact with objects
 404 around the environment.

405 3.5. Sound Synthesis

406 Sound is created due to a pressure wave propagating through
 407 a medium such as air or water. These waves are often produced
 408 by the vibrations of objects when they are struck, and human
 409 ears can convert these waves into electrical signals for the brain
 410 to process and interpret as sound. One of the most popular
 411 physically-based approaches to modeling the creation of sound
 412 is modal sound synthesis, which analyzes how objects vibrate
 413 when struck at different locations to synthesize contact sounds.

414 3.5.1. Modal Analysis and Synthesis Background

415 In order to perform modal analysis, we represent the objects
 416 using a discretized representation such as a spring-mass system
 417 or a tetrahedral mesh. The dynamics of the object can be repre-
 418 sented with the system of differential equations:

$$\mathbf{M}\ddot{\mathbf{r}} + \mathbf{C}\dot{\mathbf{r}} + \mathbf{K}\mathbf{r} = \mathbf{f} \quad (4)$$

419 \mathbf{r} is a vector of displacements from the given starting positions,
 420 which are assumed to be at rest. \mathbf{f} is the vector of external forces
 421 applied to the system. \mathbf{M} and \mathbf{K} are the mass and stiffness ma-
 422 trices, respectively, which describe the distribution of mass and
 423 connectivity of the object. For the damping matrix \mathbf{C} , we use
 424 Rayleigh damping which expresses \mathbf{C} as a linear combination
 425 of \mathbf{M} and \mathbf{K} .

426 This system of equations can be decoupled to produce a
 427 bank of modes of vibration. The equation for each mode is
 428 a standard damped oscillator, which vibrates at a certain fre-
 429 quency and decays exponentially over time. Almost all of the
 430 complex calculations are dependent only of the properties of
 431 the objects and therefore can be precomputed and stored.

432 Sound synthesis at runtime is done in two steps. When an
 433 object is struck, the modes of vibration are excited depending
 434 on the strike’s location and direction. Once the vibrations begin,
 435 the modes are sampled and updated at around 44,100 Hz to
 436 create perceptually realistic sound. For more details on modal
 437 analysis and synthesis, refer to the work of O’Brien et al. for
 438 a FEM approach using tetrahedral meshes [20] or the work of
 439 Raghuvanshi and Lin for a spring-mass approach [21].

440 3.5.2. Textures and Lasting Sounds

441 Modal synthesis works well for generating sound that varies
 442 for each object, material, and impulse. However, for long-lasting
 443 collisions such as scraping, sliding, and rolling, the sound pri-
 444 marily comes from the fine details of the surface which are not
 445 captured in the geometry of the input mesh when using texture
 446 maps. We adopt the method by Ren et al. [9], which uses three
 447 levels of detail to represent objects, with normal maps provid-
 448 ing the intermediate level of detail.

449 At the macro level, the object is represented with the pro-
 450 vided triangle mesh. The first frame in which a collision is

451 detected, it is considered transient and impulses are applied ac-
 452 cording to conventional modal synthesis. If the collision per-
 453 sists for multiple frames, we instead use the lower levels de-
 454 scribed below.

455 Even surfaces that look completely flat produce rolling, slid-
 456 ing, and scraping sounds during long-lasting collisions. The
 457 micro level of detail contains the very fine details that produce
 458 these sounds and are usually consistent throughout the material.
 459 Sound at this level is modeled as fractal noise. Playback speed
 460 is controlled by the relative velocity of the objects, and the am-
 461 plitude is proportional to the magnitude of the normal force.

462 The meso level of detail describes detail too small to be effi-
 463 ciently integrated into the triangle mesh, but large enough to be
 464 distinguishable from fractal noise and possibly varying across
 465 the surface. Normal maps contain this level of detail, namely
 466 the variation in the surface normals. This sound is produced by
 467 following the path of the collision point over time. Any time
 468 the normal vector changes, the momentum of the rolling or slid-
 469 ing object must change in order to follow the path of that new
 470 normal. This change produces an impulse which can be used
 471 alongside the others for modal synthesis. This can be mathe-
 472 matically formulated as follows.

473 Given an object with mass m moving with tangent-space ve-
 474 locity vector \mathbf{v}_t along a face of the coarse geometry with normal
 475 vector \mathbf{n}_g whose nearest normal map texel provides a sampled
 476 normal \mathbf{n}_s , the component of the momentum orthogonal to the
 477 face \mathbf{p}_n is:

$$\mathbf{p}_n = m \left(-\frac{\mathbf{v}_t \cdot \mathbf{n}_s}{\mathbf{n}_g \cdot \mathbf{n}_s} \right) \mathbf{n}_g \quad (5)$$

478 This momentum is calculated every time an object’s contact
 479 point slides or rolls to a new texel, and the difference is ap-
 480 plied as an impulse to the object. More extreme normals or a
 481 higher velocity will result in higher momentum and larger im-
 482 pulses. Whenever objects are in collision for multiple frames,
 483 both the micro-level fractal noise and the meso-level normal
 484 map impulses are applied, and the combined sound produces
 485 the long-lasting rolling, sliding, or scraping sound.

486 4. Relief Map Representation

487 As an extension to the modalities described above which
 488 rely solely on the surface’s normal vectors, we have also ex-
 489 plored how a relief map’s depth information can be incorpo-
 490 rated to improve each component. In this section, we explain
 491 these differences.

492 4.1. Modifying Collision Behavior with Relief Maps

493 When discussing rigid body physics with a normal map, we
 494 mentioned that collision *detection* remained unchanged while
 495 collision *resolution* required modification. With relief maps’
 496 depth information, collision *detection* now requires additional
 497 steps, as now objects may penetrate inside the geometry of a
 498 surface as long as they stay outside the recessed relief surface.
 499 Again focusing on the situation where a small object collides

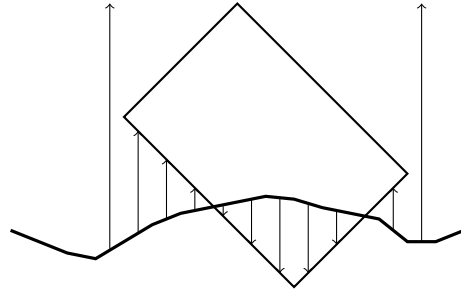


Figure 4: A rectangle colliding with a 1D relief map. Wherever arrows point downwards, the distance is negative and there is a collision.

500 with a large textured surface, the problem is collision detec-
 501 tion between an object and a height map. We adopt a similar
 502 approach described by Otaduy et al. for computing directional
 503 penetration depth between two textured objects [8].

504 In general, the penetration depth between two colliding ob-
 505 jects is the shortest distance one of the objects would have to
 506 move in order to separate themselves. The *directional* penetra-
 507 tion depth is the penetration depth where the objects can only
 508 move along one specified axis. Computing the general penetra-
 509 tion depth between finely-detailed objects can be prohibitively
 510 slow for interactive applications. Directional penetration depth
 511 can be used in place of general penetration depth, sacrificing
 512 accuracy for speed, which is more appropriate for our goals.

513 The GPU-based method proposed by Otaduy et al. for com-
 514 puting directional penetration depth is to represent each collid-
 515 ing object as a height map perpendicular to the specified direc-
 516 tion. These height maps are aligned with one another so that the
 517 distance between the objects at some point is the difference in
 518 height between two matching height map texels. Wherever the
 519 distance between objects is negative, there is a collision. The
 520 most negative distance value can then be reported as the direc-
 521 tional penetration depth.

522 In our case, the large plane textured with a relief map is al-
 523 ready a height map perpendicular to the normal vector of the
 524 plane. In order to adopt a similar technique on any CPU (and
 525 GPU), we need to convert the colliding object into a height map
 526 of its own. We primarily accomplish this by projecting the
 527 object onto the plane and rasterizing the result with the same
 528 resolution as the relief map. The depth information from that
 529 process can then be used as the object’s height map. The dif-
 530 ference between the relief map’s depth and the object’s height
 531 map is the distance between them, and one or more collision
 532 points can be found by searching for negative distances. The
 533 collision points and the normal vectors sampled from the relief
 534 map at the same locations can then be passed to the collision
 535 resolution solver.

536 A simple example is illustrated in Figure 4, where a rect-
 537 angular object is colliding with a 1D relief map. Each arrow
 538 points from a relief map texel to the corresponding texel of the
 539 rasterized object height map, where upwards arrows are posi-
 540 tive distance values and downwards arrows are negative. The
 541 most negative distance values would be reported as collision
 542 points. Since the points are found through a sampling process,

543 there is naturally a tradeoff between speed and accuracy: each
544 sample takes time to compute but contributes to finding a more
545 accurate collision point.

546 4.2. Haptic Interface with Relief Maps

547 For haptic interaction through the PHANToM, as with rigid
548 body physics, the change is in collision detection and not reso-
549 lution. The tip of the pen is projected down in the direction of
550 the surface normal, but collision is only reported if the pen’s tip
551 is below the relief map depth value. If there is a collision, the
552 simulated plane is created in exactly the same way as described
553 in the normal map section. With depth information, the pen can
554 follow the actual contours of the surface.

555 4.3. Sound Synthesis with Relief Maps

556 With normal maps, it is necessary to track the change in
557 the sampled normal vector to estimate the impulses felt by a
558 rolling, sliding, or scraping object for the purposes of sound
559 synthesis. In the case of a relief map with depth information,
560 we can compute significantly more accurate collision informa-
561 tion, and with that comes significantly more accurate impulse
562 information. With the relief map collision detection described
563 previously, we can directly take the impulses reported by the
564 physics engine and apply them to the bank of modes of vibra-
565 tion to synthesize sound.

566 Since the physics engine properly takes into account the nor-
567 mal and depth information from the relief map, the resulting
568 impulses already account for the texture detail. Adding in the
569 same fractal noise to account for surface variations too small to
570 be captured by either texture representation produces realistic
571 long-lasting contact sounds.

572 5. Implementation and Results

573 We have described each component of our multimodal sys-
574 tem using texture maps. We implemented this prototype system
575 in C++, using NVIDIA’s PhysX as the rigid body physics simu-
576 lator, OGRE3D as the rendering engine, VRPN to communi-
577 cate with the PHANToM [25], and STK for playing synthesized
578 sound [26].

579 In our previous work, we discretized our objects using spring-
580 mass systems to perform modal analysis for sound synthesis [10].
581 For this paper, we instead use a finite element method represen-
582 tation using tetrahedral meshes. The difference between the rep-
583 resentations is primarily that the spring-mass model represents
584 objects as hollow shells with a given shell thickness, while us-
585 ing tetrahedral meshes properly represents the full volume of
586 objects. With either representation, the equation in Section 3.5.1
587 is used, but matrices are constructed differently. This provides
588 an improvement in accuracy over spring-mass discretizations
589 and only negatively impacts the runtime during the precompu-
590 tation step. All scenarios we created contained at least one tex-
591 tured surface acting as the ground of the environment, and only
592 its normal map was used to modify collision response, haptic
593 display, or sound rendering.

594 5.1. Performance Analysis

595 The sound synthesis module generates samples at 44100Hz,
596 the physics engine updates at 60Hz, and while the PHANToM
597 hardware itself updates at around 1000Hz, the surface normal
598 is sampled to create a new plane once per frame. On a com-
599 puter with an Intel Xeon E5620 processor and 24GB RAM, the
600 program consistently averages more than 100 frames per sec-
601 ond. This update rate is sufficient for real-time interaction, with
602 multi-rate updates [8, 9].

603 A natural comparison is between our texture-based method
604 and methods using meshes containing the same level of detail.
605 Most of our texture maps are around 512×512 , so recreating
606 the same amount of detail in a similarly fine mesh would re-
607 quire more than $512^2 = 262114$ vertices and nearly twice as
608 many triangles. As a slightly more realistic alternative, we also
609 compare to a relatively coarse 256×256 mesh with more than
610 $256^2 = 65536$ vertices. For a discussion of LOD representa-
611 tions and the challenges in simplifying meshes for multimodal
612 systems, refer to Section 5.4.2.

613 Table 1 presents memory and timing information when com-
614 paring our method to methods using the equivalent geometry
615 meshes instead. The coarse mesh used for modal analysis is
616 greatly reduced in size compared to the finer meshes. We gen-
617 erated these finely-detailed meshes for the sake of comparison,
618 but in practice, neither mesh would be available to a game de-
619 veloper and they would have to make do with the constraints
620 considered in our method.

621 Modal analysis for audio generation on the finer meshes re-
622 quires significantly more memory than is available on modern
623 machines, so a simplified mesh is required. The listed “Run-
624 time Memory” is the runtime requirement for modal sound syn-
625 thesis and primarily consists of the matrix mapping impulses
626 to modal response. The listed memory requirements are based
627 on a spring-mass discretization for normal maps and the FEM-
628 based discretization for relief maps.

629 Our method is faster than using fine meshes in each mode
630 of interaction. Haptic rendering time using our method took
631 merely $60 \mu\text{s}$ per frame. The listed “Visual Time” is the time
632 taken to render the surface, either as a flat texture mapped plane,
633 or as a color-mapped mesh without normal mapping. The PHAN-
634 ToM’s API integrated with VRPN does not support triangular
635 meshes, and we could not test performance of collision detec-
636 tion and haptic rendering manually, though the time needed to
637 compute collision with an arbitrary triangular mesh would have
638 been significantly longer (at least by one to two orders of mag-
639 nitude based on prior work, such as H-COLLIDE).

640 The main sound rendering loop runs at around 44 kHz re-
641 gardless of the chosen representation of detail. The only differ-
642 ence comes from the source of sound-generating impulses: our
643 method for normal maps collects impulses from a path along the
644 normal map while a relief map or mesh-based approach collects
645 impulses reported by the physics engine. Applying impulses to
646 the modal synthesis system is very fast relative to the timed
647 modes of interaction.

	Mesh Size	Offline Memory	Runtime Memory	Physics Time	Visual Time	Haptic Time
Normal Map	10KB	2.7 MB	270 KB	175 μ s	486 μ s	60 μ s
Relief Map	110KB	1 GB	18 MB	2.2 ms	900 μ s	60 μ s
Coarse Mesh	4.5 MB	288 GB*	450 MB*	3.0 ms	2.1 ms	—**
Fine Mesh	19 MB	4500 GB*	1700 MB*	4.9 ms	7.0 ms	—**

Table 1: Memory and timing results for our (texture-based) methods compared to a similarly detailed coarse mesh (66,500 vertices) and fine mesh (264,200 vertices). Entries marked with * are extrapolated values, since the memory requirements are too high to run on modern machines. Haptic time (**) was not measurable for triangle meshes due to an API limitation. Normal maps are able to achieve up to **25 times** of runtime speedup and up to **6 orders of magnitude** in memory saving.

5.2. Normal Map Texture Identification User Study

In order to evaluate the effectiveness of this multimodal system, we conducted a user study consisting of a series of tasks followed by a questionnaire. One objective of this user study was to determine the overall effectiveness of our system. For this study, only the normal map representation was used. A subject is interacting with the normal map through sight, touch, and sound. If each of these components are well designed and implemented, a subject should be able to identify the material by multimodal interaction. The other goal is to see how well the use of multiple senses helps to create a cohesive recognition of the material being probed. Even if subjects find the haptic display alone is enough to understand the texture of the material being probed, does adding sound cues speed up their process of identifying textures or instead cause sensory conflict?

5.2.1. Set-up

Twelve participants volunteered to take part in this study experiment. Each subject was trained on how to use the PHANToM and was given some time to get used to the system by playing in a test scene (see Figure 7, top row). The subject then completed a series of six trials. In each trial, a material for the surface was chosen at random, and all aspects of it *except* its visual appearance were applied. That is, the subject would be able to feel the surface’s texture with the PHANToM, hear the sound generated from ball and PHANToM pen contacts, and see the rolling ball respond to ridges and valleys on the surface. The subject was able to cycle through each material’s visual appearance (in the form of a texture) by pressing the button on the PHANToM’s grip. Their task was to select the material’s unknown visual appearance based on the multimodal cues received.

The first three trials provided all three cues—sound, ball, and pen—but in each of the remaining three trials only two of the three cues would be available. The subject would be informed before the trial began if any cues were missing. The subjects were recommended to use all available cues to make their decision, but were otherwise unguided as to how to distinguish the materials. After the trials were completed, a short questionnaire was provided for subjective evaluation and feedback.

This study utilizes sensory conflict to guide the subjects to correctly identify the visual appearance. If the multimodal cues present the sounds, haptic texture, and physical response of a metal surface with regular grooves, but the subject has currently



Figure 5: The available materials for the texture identification user study. 1–3 sounded like bricks, 4–5 sounded like porcelain, 6–8 sounded like metal, and 9–10 sounded like wood.

	ID rate	Time (s)	Ease (1–10)
All modes	78%	38 \pm 18	7.9 \pm 1.3
No sound	81%	46 \pm 45	4.9 \pm 2.2
No haptics	54%	41 \pm 23	3.6 \pm 1.8
No physics	72%	47 \pm 58	6.4 \pm 2.6

Table 2: Results comparing effectiveness when limiting the available modes of interaction in the texture identification user study. “Ease” is evaluated by the subjects where 1 is difficult and 10 is easy. When using all modes of interaction, subjects were generally able to identify the material more frequently than when only using two modes and reported that they found identification to be easiest when all modalities of interaction were engaged.

selected the visual appearance of a flat, smooth wooden surface, they should recognize the sensory conflict and reject the wooden surface as the answer. Once the subject has selected the correct visual appearance (grooved metal in this example), they should feel relatively little sensory conflict and from that realize they have found the answer.

Figure 5 shows the materials chosen for the user study. The subjects were allowed to look at each of these textures before the trials began, but were not able to feel or hear them. Some of these were specifically chosen to be challenging to distinguish.

5.2.2. Experimental Results

In Table 2, we compare the results when varying which modes of interaction are available to subjects. The ID rate is the percentage of trials in which the subject was able to correctly identify the material, and the mean time only takes into

ID	Guesses (%)									
	1	2	3	4	5	6	7	8	9	10
1	50	0	33	0	0	17	0	0	10	0
2	0	80	0	20	0	0	0	0	0	0
3	0	0	100	0	0	0	0	0	0	0
4	0	0	0	83	17	0	0	0	0	0
5	0	13	25	0	50	0	12	0	0	0
6	0	0	17	0	0	83	0	0	0	0
7	8	0	8	0	0	8	60	8	8	0
8	0	0	0	0	0	0	0	75	25	0
9	0	0	17	0	0	0	0	16	67	0
10	0	0	0	0	0	0	0	0	12	88

Table 4: Confusion matrix showing the guesses made by subjects in the texture identification study. For all materials, a significant majority of subjects were able to identify the right materials.

account time for correct guesses. The “ease” was provided by the subjects on the questionnaire, where they were asked to rate on a scale from 1–10 how easy they found it was to identify the material for each combination of modes of interaction. Higher “ease” scores mean the subject found it easier to identify the material.

In all cases, the identification rate was higher than 50%, and usually much higher than that. The loss of haptic feedback caused the largest drop in ID rate and ease. The loss of sound actually improved material identification—although the difference is not statistically significant—but subjects still found identification to be much more perceptually challenging.

Two more noteworthy results were gathered from a subjective questionnaire, with results shown in Table 3. Subjects were asked how frequently they used each of the modes in identifying the material. The subjects were also asked how well each mode of interaction represented how they would expect the materials to sound or feel. These results could help explain the low identification rate when haptics are disabled: most subjects both relied heavily on tactile senses and found it be the most accurate mode. The subjects considered the sound and physics somewhat less accurate but still occasionally useful for determining the materials.

More detailed results from the study are presented in Table 4. An entry in row i and column j is the percentage of times the subject was presented material i and guessed that it was material j . The higher percentages along the diagonal demonstrate the high correct identification rate. Also note that in most categories there is no close second-place guess. The largest exception is that 33% of the time material 1 (brick grid) was mistakenly identified as material 3 (pebbles), likely due to similarity in both material sounds and patterns.

5.2.3. Analysis

Our analysis is largely based on comparing the results from interactions with different sets of modalities using a t -test to analyze the difference between the modalities. In addition to the p value for statistical significance, we also use Cohen’s effect size d , defined as the difference between the means of two samples divided by their pooled standard deviation [27]. Effect size

is an important factor to consider alongside statistical significance, explaining not just if there is a difference, but explaining (in units of standard deviations) how large that difference actually is.

Due to the relatively low sample size in the study of each material, many of the possible direct comparisons would not be statistically significant. Therefore, for this study the reported statistics are based on combined data from all study materials; we do not compare the result on each material to one another.

Between identification rates, there was no statistically significant change when removing a mode ($p > .05$), but the removal of haptics came close with $p = .066$. The subjective subject-reported values of ease and accuracy were generally more significant. Subjects reported that they found material identification to be more difficult when either sound or haptics were removed in comparison to having all modes available ($p < .05$), but did not find identification more difficult when the physics modification was removed ($p > .05$). Cohen’s effect size values (d) of 1.66 for the removal of sound and 2.79 for the removal of haptics suggest a very large change in perceptual difficulty when removing these modes. Subjects also reported that they found the haptics to be more accurate than physics or sound ($p < .05$), but did not find a significant difference in accuracy between physics and sound ($p > .05$). Cohen’s effect size values of 1.02 comparing haptics to physics and 1.36 comparing haptics to sound suggest a large difference in the perception of how accurate these modes are.

Overall, these results demonstrate that each mode of interaction is effectively enabled through use of normal maps. Combining multiple modes increases accuracy, which suggests that the subjects are receiving cohesive, non-conflicting information across their senses. This was a deliberately challenging study, using materials which sounded similar and had similar geometric features and patterns. Furthermore, the task asked subjects to carefully consider properties of materials not often noticed. Not many people take the time to consider the difference in frequency distributions between the sounds of porcelain and metal, but that distinction could have been important for these tasks. Within such a context, a 78% rate for identifying the correct material out of ten options appears rather promising, and significantly better than random selection.

5.3. Normal and Relief Comparison User Study

We now move on to discuss a second, separate user study. In order to evaluate the effectiveness of the relief map representation, we conducted another user study where subjects compared normal mapped surfaces to relief mapped surfaces. Since the previous study found most of the benefit in the subjects’ perception of the surface, this study was largely designed to test the perceptual aspects of these representations.

5.3.1. Set-up

Twenty-two subjects volunteered to participate in this study, primarily students with computer literacy in the age between 20 to 30. The subjects were allowed to interact with six textured surfaces, where, for each subject, three textures were randomly

	Always	Frequently	Occasionally	Rarely	Never	Reported accuracy (1–10)
Haptics	88%	0%	6%	0%	6%	9.3 ± 0.9
Sound	34%	22%	22%	11%	11%	7.6 ± 1.4
Physics	29%	6%	47%	6%	12%	7.3 ± 2.6

Table 3: Texture identification study: Results from question asking how often subjects used each mode of interaction and question asking how well each mode represented the materials (10 is very accurate).



Figure 6: The available materials for the normal and relief map comparison user study. Material 2 and 5 sounded like stone; 3 sounded like ceramic tile; 4 sounded like metal; 1 and 6 sounded like wood.

800 selected to use the normal map representation and the remain-
801 ing three used the relief map representation. Much like in the
802 previous user study, subjects controlled the PHANToM, which
803 corresponded to a virtual pen that could strike the surface or a
804 rolling ball. Through this interaction the subjects would feel the
805 surface, watch the ball roll across the surface, and hear sound
806 synthesized from the surface. Subjects were given as much time
807 as needed to interact with the textured surfaces, and were able to
808 switch between textures at will. Feedback was obtained through
809 a questionnaire in which subjects evaluated each texture, rating
810 the perceived realism of the visual appearance, how well each
811 mode of interaction matched what they would expect from the
812 visual appearance, and the overall quality of interaction.

813 Figure 6 shows the relief map versions of each surface cho-
814 sen for the user study. These were selected to provide a range
815 of complexity, depth, and materials. The subjects were allowed
816 to spend as much time as needed to properly evaluate each sur-
817 face.

818 The subjects were not informed that some surfaces would
819 have relief maps and some would have normal maps, nor were
820 they specifically told to consider the depth of the surface. Fur-
821 thermore, no subject ever saw both the normal and relief ver-
822 sions of the same surface, always one or the other. With the
823 subjects largely going into the study unaware of the multiple
824 representations, we pose the following questions:

- 825 • With this scenario, do the subjects find the relief maps
826 more accurate and realistic? If not, do they instead signif-
827 icantly prefer the normal maps, or are the two representa-
828 tions indistinguishable?
- 829 • Do subjects interacting with a relief mapped surface rate

830 it more highly than the subjects interacting with its nor-
831 mal map equivalent?

- 832 • How much, if any, does depth information help with re-
833 duction of sensory conflict?

834 5.3.2. Experimental Results

835 A general way to look at the results is to, for each question,
836 compare all responses (across all surface materials) to use of
837 normal maps vs. use of relief maps. This way can provide a gen-
838 eral idea of which texture representation was preferred for each
839 mode of interaction. When subjects were asked how realistic
840 the surfaces appeared, how much the ball physics matched their
841 expectations, and how much the synthesized sound matched their
842 their expectations, there was no significant difference between
843 normal maps and relief maps ($p \gg .05$). Cohen’s effect size
844 for each of these was no greater than 0.11, further indicating
845 little distinction between the texture representations.

846 When subjects were asked how well the haptics matched
847 their expectations, there was weak evidence showing that sub-
848 jects preferred the relief maps ($p \approx .053$), and Cohen’s effect
849 size of .34 indicates some moderate preference of relief maps.
850 However, when subjects reported their overall perceived qual-
851 ity of interaction, they significantly favored relief maps over
852 normal maps ($p < .05$), with Cohen’s effect size of .36 further
853 suggesting a moderate preference of relief maps.

854 In Table 5, we show the results from comparing the two ver-
855 sions of each texture to one another. For each of the six surfaces,
856 the ratings from the subjects who were given the normal map
857 version are compared to the ratings from the subjects who were
858 given the relief map version, and the table presents the p values
859 and effect sizes for each category the subjects were questioned
860 about. See the beginning of Section 5.2.3 for a brief description
861 of effect size. Notice that the results vary largely from surface
862 to surface.

863 Recall that, out of the six surfaces each subject experienced,
864 three at random were chosen to be normal maps and the other
865 three were relief maps. Comparing each subject’s average nor-
866 mal map rating to that same subject’s average relief map rating,
867 we found that each subject tended to prefer their three relief
868 maps over their three normal maps ($p < .05$).

869 5.3.3. Analysis

870 We can now revisit our originally posed questions, which
871 each involve different means of analyzing the data:

872 **Accuracy and realism of relief maps.** In order to assess the
873 overall quality of interaction with relief maps, we can consider

		Surface					
		1	2	3	4	5	6
Visuals	<i>p</i>	.03	.61	.96	.14	.21	.66
	<i>d</i>	.84	-.21	.03	.65	-.57	.18
Physics	<i>p</i>	.80	.64	.38	.83	.08	.56
	<i>d</i>	-.1	.20	-.4	.09	-.78	.25
Sound	<i>p</i>	.31	.84	.47	.27	.07	.14
	<i>d</i>	-.45	-.09	-.34	.49	-.83	.65
Haptics	<i>p</i>	.03	.70	.77	.03	.002	.002
	<i>d</i>	.9	.16	.16	1.03	-1.42	1.44
Overall	<i>p</i>	.2	.68	.92	.08	.14	.02
	<i>d</i>	.52	.18	.05	.80	-.65	1.02

Table 5: For each of the six surfaces, subjects interacted with either the normal or relief map version of that surface’s texture. This table contains results of *t*-tests for each surface and each modality determining whether there are significant differences between the subjects’ responses for each texture representation. A small *p* indicates a statistically significant difference. A positive *d* value indicates that subjects prefer the relief map version; negative indicates a preference for the normal map.

the data in aggregate, regardless of surface or user. Based on the subjects’ ratings of the surfaces’ overall quality across all surfaces, on average subjects preferred relief maps over normal maps. We also know that, despite not being informed of the multiple representations, subjects significantly preferred their three randomly selected relief maps over their three normal maps. This neglects the subjects’ opinions on individual modes of interaction, but that will be discussed later in the context of sensory conflict. When considered as a whole, relief maps were considered to be of somewhat better overall quality.

Comparisons between normal and relief map versions of the same surface. In order to see how subjects compared different versions of the same surface, we now focus on the data in Table 5, which groups ratings by surface. When broken up in this way, we now see that results varied greatly from surface to surface. For most surfaces and most modes of interaction, the differences in ratings were not statistically significant, and the effect sizes ranged from medium preference of the normal map to medium preference of the relief map. Certain textures therefore may be more suitable for representation as relief maps than others. For example, subjects often commented that haptics and ball physics were unrealistic near vertical edges in a relief map (likely due to limitations of directional penetration depth). Surface five contained many prominent near-vertical edges, and subjects strongly preferred the normal map version. Even though there is an average preference for relief maps across all surfaces, this and other situational reasons for preferring a particular representation mean that the choice of representation may need to be considered on a case-by-case basis.

Reduction of sensory conflict. In order to assess sensory conflict, we now see if the results indicate that the experience as a whole was more appealing than each separate modality would

indicate. Preferences were mixed when subjects were told to rate a specific mode of interaction, but they rated the overall quality of relief maps to be significantly higher than normal maps. This suggests that when interacting with multiple modes of interaction simultaneously, relief maps appear to produce more cohesive multimodal interaction than normal maps. Normal vectors already provided most of the cues for depth and curvature, so adding depth information in the form of a relief map only had a small effect on any one mode of interaction. It is only when all modes are considered together that the combined effect is significantly larger. While the overall quality of interaction with reliefs maps may only be moderately better on average and dependent on traits of the surface itself, this reduction in sensory conflict provides its own, possibly subconscious, advantages.

5.4. Discussion

5.4.1. Applications

We demonstrate several possibilities on the potential use of normal and relief maps as unified representations for accelerating multimodal interaction in the supplementary video. Given the prevalence of texture mapping in numerous interactive 3D graphics applications (e.g. games and virtual environment systems), our techniques enable the users to interact with textured objects that have extremely simple underlying geometry (such as flat surfaces) so that they would be able to observe consistent dynamic behaviors of moving textured objects, hear the resulting sounds from collisions between them, and feel the object contacts, as shown in Figure 7 (top row). The example of the simplified pinball game in Figure 7 (bottom right), balls rolling down Lombard Street in San Francisco City in Figure 8, and letter blocks sliding down sloped surfaces with noise or obstacles in Figure 7 are a few additional examples, where texture maps can be incorporated into physics simulation with multimodal display to provide a more cohesive, immersive experience without sensory disparity. Please see the supplementary video for demonstration of these results.

5.4.2. Comparison with Level-of-Detail Representations

While we have shown comparisons between normal maps and high-resolution meshes as representations of fine detail, using multiple levels-of-detail when appropriate can also improve runtime performance [28, 29, 30]. These LOD meshes can also reduce the complexity of the geometry while trying to retain the most important features, as determined by perceptual metrics. Since human perception is limited, there may be no significant perceptual benefit in using meshes past a certain quality, in which case the simplified version could be used throughout for significant performance gain.

However, there would be a number of challenges to overcome in designing a multimodal LOD system. The metrics defining important visual features are known to be different than the metrics defining important haptic features [31]. It remains an open problem to create metrics for selecting important audio features for switching between LODs in a multimodal system. Furthermore, the haptic LOD meshes are different from

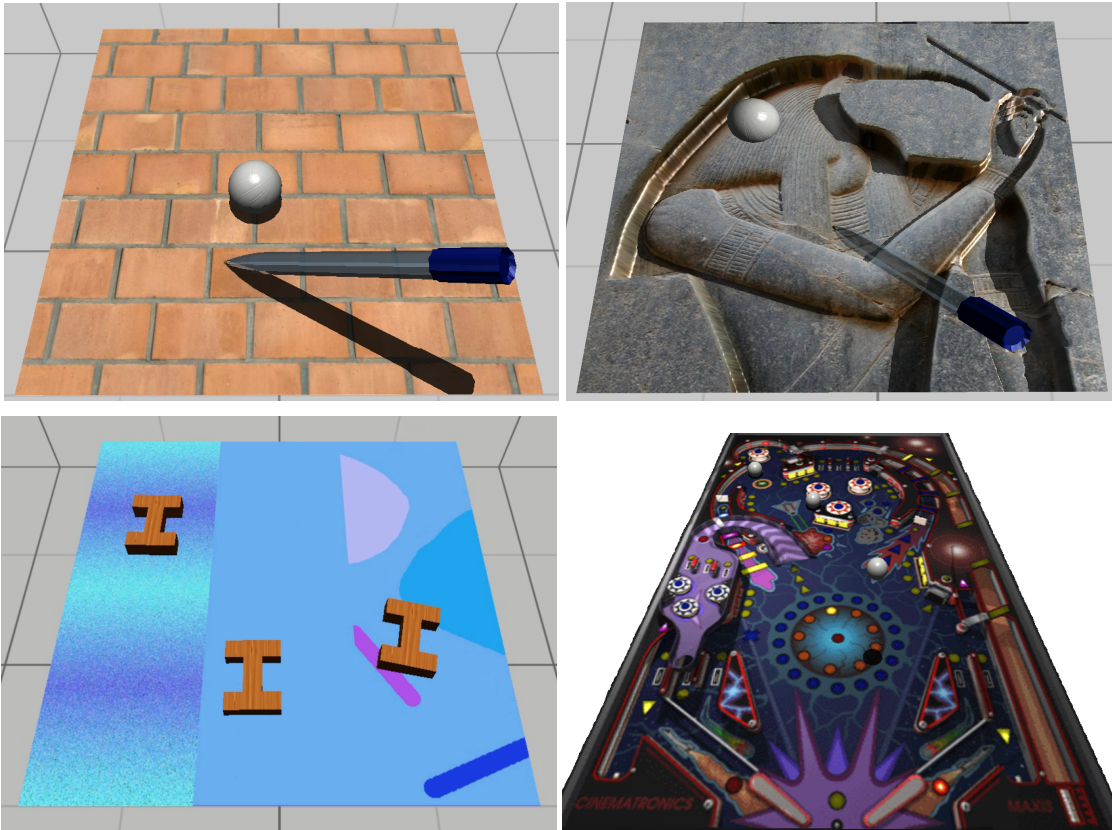


Figure 7: A selection of applications based on our system: a virtual environment with multimodal interaction with a normal map used in the texture identification user study (top left), multimodal interaction with a relief map used in the normal and relief map comparison user study (top right), letter blocks sliding down a normal-mapped surface (bottom left), and a pinball simulation on a normal-mapped flat plane (bottom right).

961 LOD meshes for visual rendering [31], leading to significantly
 962 higher memory requirements than texture-based representation
 963 in general.

964 6. Conclusion

965 In this paper, we presented an integrated system for multi-
 966 modal interaction with textured surfaces. We demonstrated that
 967 normal maps and relief maps can be used as unified representa-
 968 tions of fine surface detail for visual simulation of rigid body
 969 dynamics, haptic display and sound rendering. We showed
 970 that in a system which uses normal maps to present fine de-
 971 tail to subjects through multiple modes of interaction, subjects
 972 are able to combine this information to create a more cohesive
 973 mental model of the material they are interacting with. Our first
 974 user evaluation result further provides validation that our sys-
 975 tem succeeded in reducing sensory conflict in virtual environ-
 976 ments when using texture maps. Our second user evaluation re-
 977 sult demonstrates that relief maps, when chosen carefully, may
 978 produce a further reduction in sensory conflict.

979 We have now explored two different texture representations
 980 of fine detail, but some limitations should be addressed. Our
 981 current implementation and studies limited the texture-mapped
 982 surfaces to single flat planes and we assume our multimodal
 983 method would translate gracefully to more complex shapes, as
 984 techniques exist for *visually* rendering relief maps on arbitrary
 985 polygonal surfaces [7]. We have also only been detecting col-

986 lisions between static relief-mapped surfaces and dynamic *non-*
 987 *relief-mapped* objects. A more generalized and versatile system
 988 could consider the texture of both colliding textured objects,
 989 even if both are dynamic, although performance may become
 990 more of a limitation. Vectorial textures may be used to help
 991 reducing the aliasing artifacts of relief maps in better render-
 992 ing sharp edges. Additionally, our choice of haptic device has
 993 limited our results to 3-DOF force feedback, though it should
 994 be possible to compute torques with a slight extension of our
 995 method.

996 For future research, it may be possible to explore the inte-
 997 gration of material perception [32, 33] for multimodal displays
 998 based on some of the principles described in this paper. Future
 999 work may also attempt to generalize this system by addressing
 1000 the limitations described. We hope this work will lead to further
 1001 interest in development of techniques on minimizing sensory
 1002 conflicts when using texture representations for interactive 3D
 1003 graphics applications, like AR and VR systems.

1004 Acknowledgments

1005 This research is supported in part by National Science Founda-
 1006 tion and the UNC Arts and Sciences Foundation.

- 1007 [1] Cook RL. Shade trees. In Proceedings of the 11th Annual Confer-
 1008 ence on Computer Graphics and Interactive Techniques. SIGGRAPH
 1009 '84; New York, NY, USA: ACM. ISBN 0-89791-138-5; 1984,
 1010 p. 223–31. URL: <http://doi.acm.org/10.1145/800031.808602>.
 1011 doi:10.1145/800031.808602.



Figure 8: Lombard street color map with normal map (left) and mapped to a plane with rolling balls (right).

- [2] Blinn JF. Simulation of wrinkled surfaces. SIGGRAPH Comput Graph 1978;12(3):286–92. URL: <http://doi.acm.org/10.1145/965139.507101>. doi:10.1145/965139.507101.
- [3] Cohen J, Olano M, Manocha D. Appearance-preserving simplification. In Proceedings of the 25th Annual Conference on Computer Graphics and Interactive Techniques. SIGGRAPH '98; New York, NY, USA: ACM. ISBN 0-89791-999-8; 1998, p. 115–22. URL: <http://doi.acm.org/10.1145/280814.280832>. doi:10.1145/280814.280832.
- [4] Kaneko T, Takahei T, Inami M, Kawakami N, Yanagida Y, Maeda T, et al. Detailed shape representation with parallax mapping. In Proceedings of the ICAT. 2001, p. 205–8.
- [5] Tevs A, Ihrke I, Seidel HP. Maximum mipmaps for fast, accurate, and scalable dynamic height field rendering. In Proceedings of the 2008 Symposium on Interactive 3D Graphics and Games. I3D '08; New York, NY, USA: ACM. ISBN 978-1-59593-983-8; 2008, p. 183–90. URL: <http://doi.acm.org/10.1145/1342250.1342279>. doi:10.1145/1342250.1342279.
- [6] Oliveira MM, Bishop G, McAllister D. Relief texture mapping. In Proceedings of the 27th Annual Conference on Computer Graphics and Interactive Techniques. SIGGRAPH '00; New York, NY, USA: ACM Press/Addison-Wesley Publishing Co. ISBN 1-58113-208-5; 2000, p. 359–68. URL: <http://dx.doi.org/10.1145/344779.344947>. doi:10.1145/344779.344947.
- [7] Policarpo F, Oliveira MM, Comba JaLD. Real-time relief mapping on arbitrary polygonal surfaces. In Proceedings of the 2005 Symposium on Interactive 3D Graphics and Games. I3D '05; New York, NY, USA: ACM. ISBN 1-59593-013-2; 2005, p. 155–62. URL: <http://doi.acm.org/10.1145/1053427.1053453>. doi:10.1145/1053427.1053453.
- [8] Otaduy M, Jain N, Sud A, Lin M. Haptic display of interaction between textured models. In IEEE Visualization Conference. 2004, p. 297–304. doi:10.1109/VISUAL.2004.37.
- [9] Ren Z, Yeh H, Lin M. Synthesizing contact sounds between textured models. In Virtual Reality Conference (VR), 2010 IEEE. 2010, p. 139–46. doi:10.1109/VR.2010.5444799.
- [10] Sterling A, Lin MC. Integrated multimodal interaction using normal maps. In Proceedings of the 41st Graphics Interface Conference. GI '15; Toronto, Ont., Canada, Canada: Canadian Information Processing Society. ISBN 978-0-9947868-0-7; 2015, p. 33–40. URL: <http://dl.acm.org/citation.cfm?id=2788890.2788898>.
- [11] Szirmay-Kalos L, Umenhoffer T. Displacement mapping on the GPU - State of the Art. Computer Graphics Forum 2008;27(1).
- [12] Nykl S, Mourning C, Chelberg D. Interactive mesostructures. In Proceedings of the ACM SIGGRAPH Symposium on Interactive 3D Graphics and Games. I3D '13; New York, NY, USA: ACM. ISBN 978-1-4503-1956-0; 2013, p. 37–44. URL: <http://doi.acm.org/10.1145/2448196.2448202>. doi:10.1145/2448196.2448202.
- [13] Ho CH, Basdogan C, Srinivasan M. A ray-based haptic rendering technique for displaying shape and texture of 3d objects in virtual environments. In ASME Winter Annual Meeting. 1997,.
- [14] Ho CH, Basdogan C, Srinivasan MA. Efficient point-based rendering techniques for haptic display of virtual objects. Presence: Teleoper Virtual Environ 1999;8(5):477–91. URL: <http://dx.doi.org/10.1162/105474699566413>. doi:10.1162/105474699566413.
- [15] Theoktisto V, Gonzalez MF, Navazo I. Hybrid rugosity mesostructures (hrms) for fast and accurate rendering of fine haptic detail. CLEI Electron J 2010;:-1.
- [16] Galoppo N, Tekin S, Otaduy MA, Gross M, Lin MC. Interactive haptic rendering of high-resolution deformable objects. In Proceedings of the 2Nd International Conference on Virtual Reality. ICVR'07; Berlin, Heidelberg: Springer-Verlag. ISBN 978-3-540-73334-8; 2007, p. 215–33. URL: <http://dl.acm.org/citation.cfm?id=1770090.1770116>.
- [17] Minsky M, Ming Oy, Steele O, Brooks Jr. FP, Behensky M. Feeling and seeing: Issues in force display. SIGGRAPH Comput Graph 1990;24(2):235–41. URL: <http://doi.acm.org/10.1145/91394.91451>. doi:10.1145/91394.91451.
- [18] Minsky MDRR. Computational haptics: The sandpaper system for synthesizing texture for a force-feedback display. Ph.D. thesis; Cambridge, MA, USA; 1995. Not available from Univ. Microfilms Int.
- [19] van den Doel K, Pai DK. The sounds of physical shapes. Presence 1996;7:382–95.
- [20] O'Brien JF, Shen C, Gatchalian CM. Synthesizing sounds from rigid-body simulations. In Proceedings of the 2002 ACM SIGGRAPH/Eurographics Symposium on Computer Animation. SCA '02; New York, NY, USA: ACM. ISBN 1-58113-573-4; 2002, p. 175–81. URL: <http://doi.acm.org/10.1145/545261.545290>. doi:10.1145/545261.545290.
- [21] Raghuvanshi N, Lin MC. Interactive sound synthesis for large scale environments. In Proceedings of the 2006 Symposium on Interactive 3D Graphics and Games. I3D '06; New York, NY, USA: ACM. ISBN 1-59593-295-X; 2006, p. 101–8. URL: <http://doi.acm.org/10.1145/1111411.1111429>. doi:10.1145/1111411.1111429.
- [22] Doel KVD, Kry PG, Pai DK. Foleyautomatic: Physically-based sound effects for interactive simulation and animation. In in Computer Graphics (ACM SIGGRAPH 01 Conference Proceedings. ACM Press; 2001, p. 537–44.

- 1104 [23] Hayward V. A brief taxonomy of tactile illusions and
1105 demonstrations that can be done in a hardware store.
1106 *Brain Research Bulletin* 2008;75(6):742–52. URL:
1107 <http://www.sciencedirect.com/science/article/pii/S0361923008000178>.
1108 doi:<http://dx.doi.org/10.1016/j.brainresbull.2008.01.008>;
1109 special Issue: Robotics and Neuroscience.
- 1110 [24] Massie TH, Salisbury JK. The phantom haptic interface: A device for
1111 probing virtual objects. In *Proceedings of the ASME winter annual meet-*
1112 *ing, symposium on haptic interfaces for virtual environment and teleoper-*
1113 *ator systems*; vol. 55. Chicago, IL; 1994, p. 295–300.
- 1114 [25] Taylor II RM, Hudson TC, Seeger A, Weber H, Juliano J, Helser AT.
1115 *Vrpn: a device-independent, network-transparent vr peripheral system.*
1116 In *Proceedings of the ACM symposium on Virtual reality software and*
1117 *technology*. ACM; 2001, p. 55–61.
- 1118 [26] Cook PR, Scavone GP. The synthesis toolkit (stk). In *Proceedings of*
1119 *the International Computer Music Conference*. 1999,.
- 1120 [27] Nakagawa S, Cuthill IC. Effect size, confidence inter-
1121 val and statistical significance: a practical guide for biol-
1122 ogists. *Biological Reviews* 2007;82(4):591–605. URL:
1123 <http://dx.doi.org/10.1111/j.1469-185X.2007.00027.x>.
1124 doi:10.1111/j.1469-185X.2007.00027.x.
- 1125 [28] Otaduy MA, Lin MC. Sensation preserving simplification for haptic ren-
1126 dering. *ACM Trans on Graphics (Proc of ACM SIGGRAPH)* 2003;;543–
1127 53.
- 1128 [29] Otaduy MA, Lin MC. CLODs: Dual hierarchies for multiresolution
1129 collision detection. *Eurographics Symposium on Geometry Processing*
1130 2003;;94–101.
- 1131 [30] Yoon S, Salomon B, Lin MC, Manocha D. Fast collision detection be-
1132 tween massive models using dynamic simplification. *Eurographics Sym-*
1133 *posium on Geometry Processing* 2004;;136–46.
- 1134 [31] Otaduy MA, Lin MC. Sensation preserving simplifica-
1135 tion for haptic rendering. In *ACM SIGGRAPH 2005*
1136 *Courses*. SIGGRAPH '05; New York, NY, USA: ACM;
1137 2005,URL: <http://doi.acm.org/10.1145/1198555.1198607>.
1138 doi:10.1145/1198555.1198607.
- 1139 [32] Ren Z, Yeh H, Klatzky R, Lin MC. Auditory perception of geometry-
1140 invariant material properties. *Proc of IEEE VR* 2013;.
- 1141 [33] Ren Z, Yeh H, Lin MC. Example-guided physically-based modal sound
1142 synthesis. *ACM Trans on Graphics* 2013;32(1):Article No. 1.